Subjective and Objective Workload Assessment of Novel Autorotation Cueing Methods using Haptic Cues

Mushfiqul Alam, Cranfield University, Centre for Aeronautics, Bedford, United Kingdom
Wajih Memon, The University of Liverpool, United Kingdom
Michael Jump, The University of Liverpool, Liverpool, United Kingdom

Abstract

The helicopter autorotation manoeuvre is an emergency flight manoeuvre used primarily to safely land in the event of a main rotor engine failure. Executing this manoeuvre is challenging because pilots must perform multiple tasks simultaneously, each with precise timing. Accidents, some fatal, continue to occur when carrying out an autorotation manoeuvre and these are generally attributed to pilot error. There is therefore a recognised need to develop a system to aid pilots to perform a safe, survivable autorotation. As part of a wider project to develop novel autorotation cueing methods by the authors, several piloted simulated trials had been conducted using the University of Liverpool's HELIFLIGHT-R full motion simulator. This paper reports on an investigation into the potential correlation between subjective workload metrics collected during those trials and objective measures which look promising as a surrogate for workload. Subjective workload was collected using the Bedford Workload Rating Scale. The objective assessment used was the weighted combined multi-axis attack activity rate developed at the University of Liverpool. Three different initial start conditions for the autorotation manoeuvre with and without haptic cueing in a good visual environment condition were tested. It was hypothesised that the subjective workload ratings would be well correlated with one or both of the average or peak multi-axis attack activity rates for the phase of the manoeuvre under consideration. However, no correlation was found between either the combined multi-axis localised average or peak attack activity and the subjective workload reported by the test pilots.

NOTATION

Symbols

A_η	Control attack parameter (for control input η), per s
$A_{\eta N}$	Number of control attack points, -
$A_{\eta R}$	Control activity rate, per s
$A_{\eta RC}$	Combined weighted adaptive attack activity rate for all four controls, per s
XA, XB, XC, XP	Lateral, longitudinal, collective and pedal control input, %
η	Pilot control deflection, %

Subscripts

i	Four XA, XB, XC, XP controls
avg	Average control attack activity rate
pk	Peak control attack activity rate

Acronyms

BWRS	Bedford Workload Rating Scale
HUD/HDD	Head Up, Head Down Display
MTE	Mission Task Element
RPM	Revolutions Per Minute
STFT	Short-Time Fourier Transform
TP	Test Pilot

1. INTRODUCTION

Autorotation for helicopters is an emergency flight manoeuvre used primarily to safely land the aircraft in the event of a main rotor engine failure [1]. Executing this manoeuvre is challenging because pilots must perform multiple tasks simultaneously, each with precise timing. Pilot feedback indicates that they generally prefer to conduct the autorotation manoeuvre with eyes out of the cockpit, perhaps for obvious reasons. Several accidents have occurred when carrying out autorotation manoeuvres, both in real and practice scenarios, due to pilot error, for example Ref [2]. Hence, there is a recognised need to develop a system to aid pilots to perform a safe, survivable autorotation. As part of a wider project to develop novel autorotation cueing methods, several piloted simulated trials had been conducted using the University of Liverpool's HELIFLIGHT-R full motion simulator. These included the use of a Head Up Display (HUD), Head Down Display (HDD) and haptic cueing [3–5]. The haptic cues were provided through the longitudinal and collective stick positions, XB and XC.

During these simulator studies both with and without haptic cues, subjective workload ratings were collected by the authors using the Bedford Workload Rating Scale (BWRS) [6] (see Appendix A). The pilots were first asked to provide overall BWRS ratings for two phases of the manoeuvre (engine failure to steady state capture and then for the steady state descent), and secondly to provide BWRS ratings in relation to maintaining the main rotor RPM and the forward airspeed during each of the phases. One of the key results from this work was that pilots reported a higher workload when performing the autorotation manoeuvre without cues [3–5] compared to when they were assisted by the haptic cues provided to them [4] to help maintain the main rotor and forward airspeeds. However, the overall BWRS ratings from the pilots did not show that the pilot workload was reduced by the haptic cues. This was despite them providing comments that indicated that they were in favour of the collective cueing in particular.

In the prior work reported in Ref [7], it was shown that the objective metrics of the Pilot Attack, A_η parameter or one of its derivatives can be used to correlate the Handling Qualities Rating (HQR) awarded by the pilots for the Mission Task Elements (MTE) listed in the Aeronautical Design Standard (ADS)–33E [1] such as the Precision Hover, Pirouette and Roll-Step. The Pilot Attack metric, A_η, is based on the rate and magnitude of the pilot's control input along the lines of the attitude quickness parameter to quantify agility [8]. The rationale here is that it is assumed that pilots will experience higher workload the more active they are on the control inceptors. It was shown that the peak and average attack metrics (discussed further in Section 4) had the strongest correlation with the HQR for tasks defined in ADS-33.

An HQR is not a direct measure of workload, but it is related to it. Each task will have an inherent workload associated with it, but a vehicle with poor handling qualities will attract a higher HQR assuming that the pilot has to apply more compensation to achieve the same standards in the task when compared to using a vehicle with 'better' handling qualities. For the autorotation study, the same aircraft model was used throughout and so it was assumed that any differences in subjective workload ratings would be due to the absence or inclusion of the cues provided. Therefore, given the correlation between HQRs and Attack Parmeter, it was hypothesised that the subjective workload ratings from the BWRS for the autorotation test points might correlate to the objective workload, calculated using the Pilot Attack parameter or one of its derivatives [7,9]. In the current study, an objective analysis of pilot workload to perform an autorotation manoeuvre is conducted to investigate whether or not the overall subjective workload reported by the test pilots (TPs) for the autorotation manoeuvre is related to pilot control activity via the Attack Parameter and its derivatives.

The remainder of the paper is organised as follows: Section 2 presents the experimental setup used for the simulated autorotation manoeuvres. Section 3 introduces the Pilot Attack parameters used for the analysis as well as the other methodologies used in the investigation. Section 4 presents the results of the subjective pilot workload ratings reported by the test pilots during the autorotation manoeuvres and contrasts them with the results of the corresponding objective analyses. Finally, conclusions are presented in Section 5.

2. EXPERIMENTAL SET-UP

Figure 1. HELIFLIGHT-R flight simulator.

Simulated pilot-in-the-loop autorotation manoeuvre test campaigns were performed using the University of Liverpool's HELIFLIGHT-R full-motion simulation facility [10], Figure 1. The FLIGHTLAB non-linear generic rotorcraft flight dynamics model (based upon a UH-60 Black Hawk) was used in these simulated flight tests. Three Test Pilots (TP) were used for the simulator test campaigns. TP1 is a former Royal Air

Force helicopter squadron pilot as well as a former tutor and commander of the Empire Test Pilot School (ETPS). TP2 is a former Royal Navy rotary wing pilot, a graduate of ETPS and a current Training Captain with a national flag-carrier airline. TP3 is an ex-Royal Air Force rotary wing pilot and a graduate of the French Test Pilot School (EPNER) and was an experimental test pilot for offshore helicopter operations.

2.1. Haptic Cueing

Pilots were provided with haptic cues in the form of a stick shaker on both the longitudinal cyclic and collective sticks. The haptic cues were provided to alert the pilot to high or low main rotor RPM on the collective and high or low airspeed on the longitudinal cyclic. Cueing as to whether a parameter was high or low and its proximity to the warning boundary was provided by varying both the frequency and amplitude of the stick-shake oscillation. Following discussions with the test pilots, the haptic cues were not active at or below 150ft above ground level. This is the approximate expected height for the entry to the flare portion of the manoeuvre and there was a concern that the haptic cueing would become a nuisance in this phase.

Table 1 shows the envelope of protection provided for the main rotor RPM cueing as well as the associated stick shaker parameters. Table 2 shows the corresponding parameters for the longitudinal cyclic forward speed cueing, noting that the nominal airspeed for the autorotation was 80 knots. It should be further noted that the ‘Amplitude’ parameter does not correspond to a physical quantity and so the magnitude of the stick shakes should be considered relative to one another. The value used was set empirically using a fourth test pilot’s opinion/feedback during the experimental set-up phase of the project. Having been involved in the experimental set-up, this pilot was not used in the main experimental test campaign.

2.2. Pilot Tasks

In all of the prior work for this project, the aircraft heading has been aligned with the runway centreline and so the autorotation manoeuvre was flown ‘straight in’ to the runway. However, this task rarely resulted in the kind of deviations from either main rotor RPM or forward speed detailed in Table 1 or Table 2. To ascertain the efficacy of the stick shaker cue across as wide a range of deviations from nominal as possible, alternatives to this original test case were therefore devised in collaboration with the test pilots. Figure 2 and The secondary task was then to maintain both indicated airspeed and main rotor speed within the nominal limits specified in Table 1 and Table 2. Engine failure was simulated by disengaging the clutch from the main rotor in the helicopter model.

Table 3 show the start conditions for the 3-autorotation manoeuvres that the pilots were asked to perform. In each case, the pilot’s task was to land ‘safely’ on the runway within the limits specified in Table 4 [11] (the runway at Liverpool John Lennon airport is 2285m in length).

Table 1. Main rotor RPM stick shaker limits & characteristics.

Limit	Main Rotor RPM (%)	Shake Frequency (Hz)	Shake Amplitude (-)
Never Exceed	≥120	20	30
Upper Limit 2	110 – 120	20	30
Upper Limit 1	105 – 110	20	15
Nominal	95 – 105	0	0
Lower Limit 1	90 – 95	5	2
Lower Limit 2	80 - 90	5	5
Never go below	≤80	5	15

Table 2. Airspeed sticks shake limits & characteristics.

Limit	Airspeed (kts)	Shake Frequency (Hz)	Shake Amplitude (-)
Upper Limit	≥90	10	5
Nominal	75 – 90	0	0
Lower Limit	≤75	10	5

Table 2

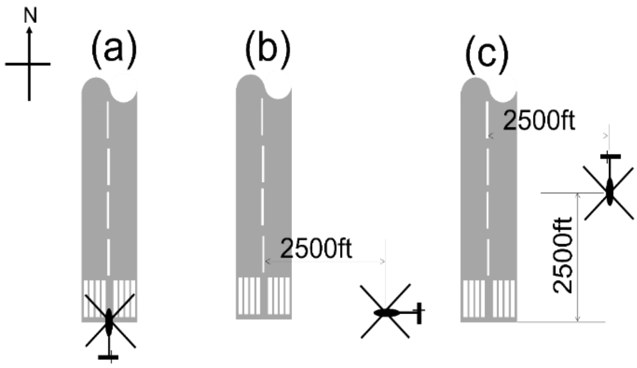

Figure 2. Autorotation manoeuvre test point start locations.

The secondary task was then to maintain both indicated airspeed and main rotor speed within the nominal limits specified in Table 1 and Table 2. Engine failure was simulated by disengaging the clutch from the main rotor in the helicopter model.

Table 3. Autorotation manoeuvre test point initial conditions.

Case	Initial Airspeed (kt)	Heading (°)	Altitude AGL (ft)
(a)	100	360	2000
(b)	100	270	2000
(c)	100	180	2000

Table 4. Autorotation manoeuvre successful touchdown definition.

Parameter	Value
Pitch angle	<12°
Forward speed	<30kts
Vertical speed	<15ft/s
Pitch rate	-30°/s - 20°/s

For the manoeuvres specified in Figure 2 and Table 3, scenario (a) was therefore a straight-in autorotation landing manoeuvre, scenario (b) required a 90° turn to the right and scenario (c) required a 180° turn to land on the northerly runway heading. As previously noted, the desired steady-state autorotation speed was 80 knots. As such, the start condition airspeed for each test case was deliberately set to be 'off nominal condition'.

2.3. Pilot Rating Scale

Following the completion of each test point, the pilots were asked to provide ratings using the BWRS [6].

Because the haptic system was switched off for the flare phase of the manoeuvre, these results were provided only for the first two phases of the autorotation manoeuvre, viz:

i. Engine failure to stabilization (entry to the steady state descent phase) and

ii. Steady-state descent.

In order to be confident in the ratings awarded, each pilot was given the opportunity to fly a given test point as often as they felt necessary before providing the rating for it.

3. DEVELOPMENT OF OBJECTIVE WORKLOAD MEASURE USING PILOT ATTACK

This section presents the fundamentals of Pilot Attack parameter as an objective workload measure.

3.1. Control Attack

The control attack or pilot attack parameter, A_η characterises each discrete control input and is defined as the ratio of the peak rate of control displacement ($\dot{\eta}_{pk}$) to the magnitude of the change in the control displacement ($\Delta\eta$) given by:

(1) $$A_\eta = \frac{\dot{\eta}_{pk}}{\Delta\eta}$$

In broad terms, higher attack values indicate rapid-small control deflections while a lower attack value indicates slower-large control deflections. Similar to the attitude quickness parameter defined within the Aeronautical Design Standard (ADS)–33 [1], the control attack parameter approximates the inverse of the time to change for a simple ramp.

The pilot attack A_η can be further quantified using the two metrics derived from A_η; first the Attack Number ($A_{\eta N}$) and second the Attack Activity Rate ($A_{\eta R}$). These are defined as:

i. Attack Number ($A_{\eta N}$): the total number of times that the pilot displaces a particular control having a magnitude higher than a specified threshold value. Discussion on the appropriate value of the attack thresholds comes later in this section.

ii. Attack Activity Rate ($A_{\eta R}$): the ratio of the total number of A_η to the time taken to complete a given task. It can be defined as the 'busyness' metric and an average for the task.

3.2. Control Attack Threshold

When assessing different attack-based metrics to examine correlations with workload ratings awarded by a pilot, it is important to determine a threshold value for what might be described as a productive pilot control input. The details on how to select this threshold value can be found in Ref. [7]. The analysis of Reference [7] showed that a threshold value of 2.5% appropriately captured the attack points with the control activity that was needed to complete a task in a manoeuvre. In this paper, a threshold value of 2.5% of the full control travel range is used (-50 to 50% for XA, XB and XP; 0 to 100% for XC).

3.3. Time-Varying Localised Attack Activity Rate

Reference [7] further showed that the peak and average attack activity rate parameter, $A_{\eta R}^{pk}$ and $A_{\eta R}^{avg}$, can be used to correlate with the HQR for tasks such as Precision Hover, Pirouette, Roll-Step, etc.. If an average $A_{\eta R}$ is used for the whole phase of the autorotation manoeuvre (engine failure to stabilization or steady-state descent) it can be difficult to identify the sections within each flight phases where the pilot was working the hardest. To capture the local peaks in $A_{\eta R}$ within each flight phase of the manoeuvre, a time-varying attack activity rate metric (${A_{\eta R}}^{loc}$) was utilised. Using a 5s window, a control segmentation approach was formulated with 2.5s overlap. The 5s window was selected based on the minimum time needed for the pilot to perceive visual cues and successfully execute a manoeuvre [12].

3.4. Time-Frequency Domain and Attack-Rate Metric Composite

A time-frequency domain (TFD) and time-varying attack activity rate metric (${A_{\eta R}}^{loc}$), TFD-${A_{\eta R}}^{loc}$, chart is created to demonstrate the applicability of the $A_{\eta R}$ metric in assessing pilot workload. A TFD is a Fourier transform-based spectrogram. A spectrogram is a three-dimensional visual representation of the frequency spectrum within the signal (in the case of this paper, the control input) as a function of time [13] and magnitude of the amplitude of the signal. TFD-${A_{\eta R}}^{loc}$ can be used to understand the pilot's control activity and transition to using different control inputs in different phases of the manoeuvre.

The spectrogram contour-plot shows the time and frequency on the abscissa and ordinate, respectively, with the colour bar indicating the magnitude of the Short-Time Fourier Transform (STFT) of the control signal. The spectrogram is formulated using a moving 4s window was selected to provide a suitable resolution in both time and frequency to highlighting key features.

An example autorotation trajectory flown by TP1 for the 90^o right turn scenario with no cue is shown in Figure 3, for the full aircraft states for this test point, see Appendix B.

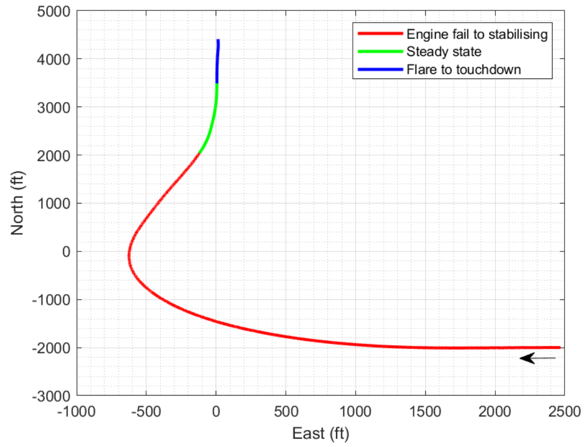

(a) Autorotation trajectory, North-East.

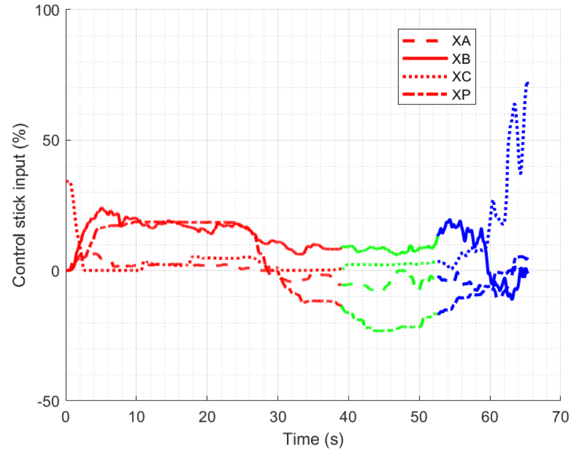

(b) Pilot's control inputs.

Figure 3. Autorotation trajectory for 90^o turn with no cue for TP1.

It can be seen in Figure 3b that, from 0 to 5 seconds, just after the engine is failed, the pilot lowered the collective (XC) and tried to stabilise the forward speed by using longitudinal cyclic (XB). In addition, the pilot initiates a right-hand turn using the pedals (XP). Once the steady state is established, the pilot makes minor adjustments to the control inceptor positions to maintain the steady state descent.

A TFD-${A_{\eta R}}^{loc}$ chart shown in

Figure *4* consists of, first a central plot contains the spectrogram of the individual control input showing the time and frequency on the abscissa and ordinate, respectively, with the colour bar indicating the magnitude of the Short-Time Fourier Transform (STFT) of the control signal; second the outer plots show the time history (upper); third, the Fast Fourier Transform (FFT) (left) and fourth, the ${A_{\eta R}}^{loc}$ (lower).

Figure *4* shows an example TFD-${A_{\eta R}}^{loc}$ chart for the four control input channels for the example trajectory shown in Figure 3.

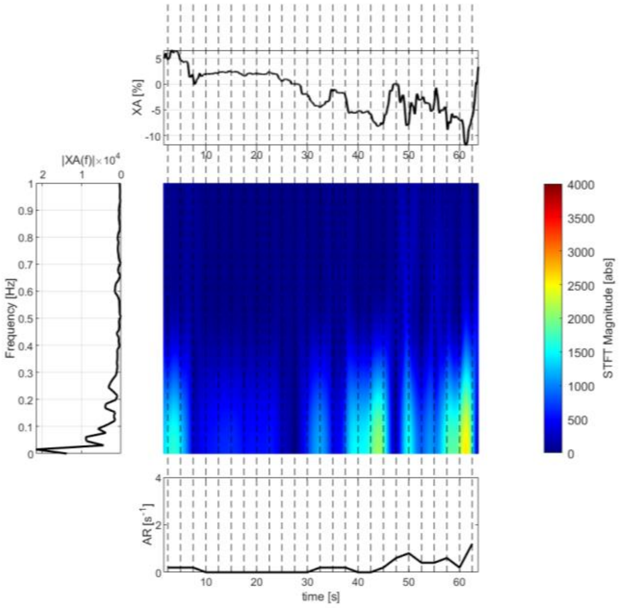

(a) TFD-${A_{\eta R}}^{loc}$ for XA.

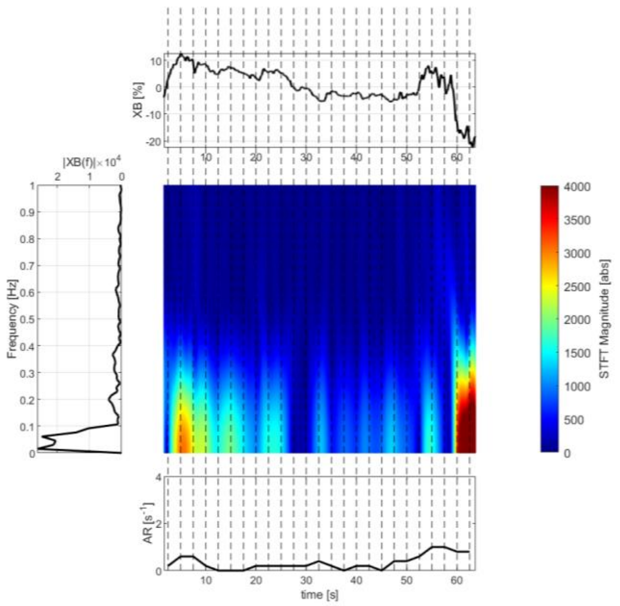

(b) TFD-${A_{\eta R}}^{loc}$ for XB.

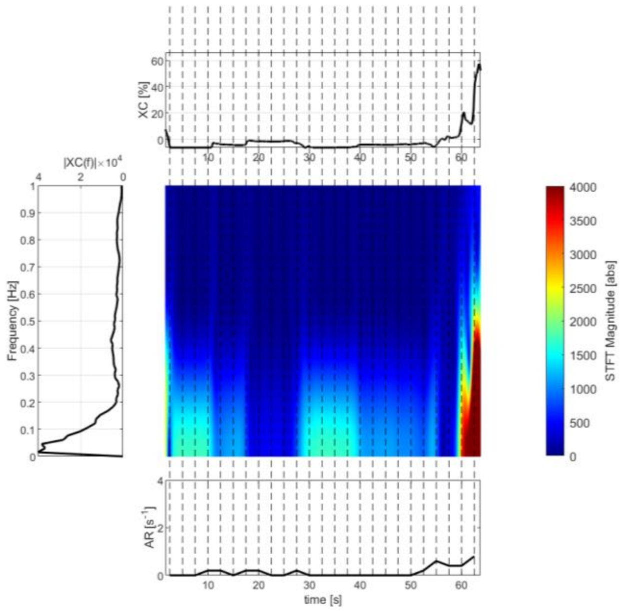

(c) TFD-${A_{\eta R}}^{loc}$ for XC.

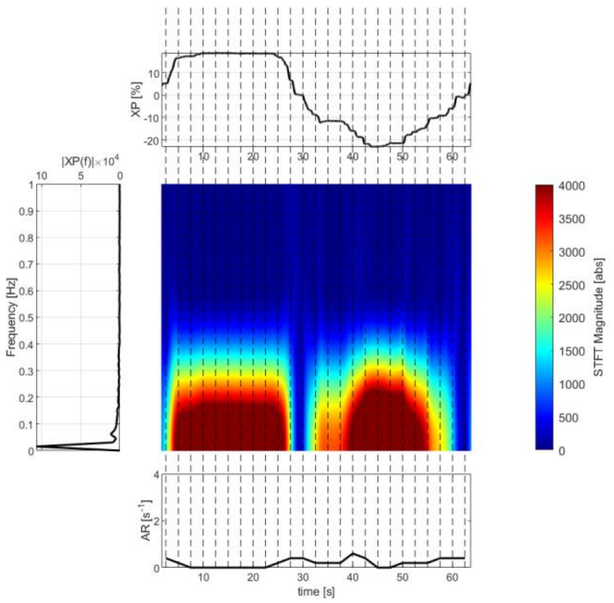

(d) TFD-${A_{\eta R}}^{loc}$ for XP.

Figure 4. TFD-${A_{\eta R}}^{loc}$chart for the control activity of the TP1.

Using the TFD-${A_{\eta R}}^{loc}$charts shown in

Figure *4*, details regarding the control activity in the different phases of the autorotation manoeuvre can be observed along with the information for the frequency content as a function of time. In the engine fail to stabilisation phase (approximately between 0 to 40 seconds), the FFT shows there is a dominant peak frequency of around 0.02Hz in the XP channel with a large peak magnitude around 4000 (red regions in

Figure *4*d) which corresponds to approximately 0 to +20% input from the pedals (upper plot in

Figure *4*d), and dominant peak frequency at around 0.08Hz in the XB channel with dominant peak magnitude around 2500 (yellow regions in

Figure *4*b) which corresponds to 0 to +10% control input in the XB channel (upper plot in

Figure *4*b), and dominant peak frequency at 0.05Hz with a dominant peak magnitude at 1500 in the XC channel (cyan region in

Figure *4*c) which corresponds to 15% to 0% control input in XC channel (upper plot in

Figure *4*c) . The XA channel during this phase has a maximum value of around 1000 (blue regions, see

Figure *4*a) which corresponds to control input of 5% to 0% in the XA channel (upper plot in

Figure *4*a), meaning the activity was low in this channel compared to the others.

During the steady state phase of the flight, the control activity remains low in the XA, XB and XC channels. Some elevated activity can be seen in the XC channel (the red region from time 40 to 55 seconds in

Figure *4*d). From the pilot's account of the task, the TP was trying to align the helicopter with the runway centreline using the pedals.

The spectrogram and ${A_{\eta R}}^{loc}$ variations show where in the manoeuvre the TP was using higher control inputs.

3.5. Combined multi-axis attack activity rate metric

Following the work presented in Ref [7] to capture the multi-axis control activity, a combined weighted adaptive metric $A_{\eta RC}$ is used calculated from the ${A_{\eta R}}^{loc}$ of individual control axis. Two values obtained from $A_{\eta RC}$ are used for comparison of subjective workload, first the average combined multi-axis activity rate, $A_{\eta RC}^{avg}$ and second the peak combined multi-axis activity rate $A_{\eta RC}^{pk}$.

The average combined multi-axis activity rate, $A_{\eta RC}^{avg}$ is calculated using Eq. 2.

$$A_{\eta RC}^{avg} = \sum_{i=XA}^{XP} {A_{\eta R_i}}^{loc} W_i^{avg} \quad (2)$$

Here i corresponds to the four-control inputs (XA, XB, XC and XP). The adaptive weight (W_i^{avg}) for each axis is calculated using the individual control's ${A_{\eta R}}^{loc}$ contribution with the corresponding fraction of total control attacks ($A_{\eta NTot}$) applied in that axis shown in Eq. 3.

$$W_i^{avg} = \frac{A_{\eta N_i}}{A_{\eta NTot}} \quad (3)$$

The peak combined multi-axis activity rate, $A_{\eta RC}^{pk}$ is calculated using Eq.4.

$$A_{\eta RC}^{pk} = \sum_{i=XA}^{XP} \overline{{A_{\eta R_i}}^{loc}} W_i^{pk} \quad (4)$$

Here $\overline{A_{\eta R_{\iota}}}^{loc}$ is the peak value of $A_{\eta R}{}^{loc}$ obtained from the TFD-$A_{\eta R}{}^{loc}$ chart (discussed in Section 3.4) for which the STFT magnitude value is the highest. The adaptive weight W_i^{pk} is calculated using Eq. 5.

$$W_i^{pk} = \frac{\overline{A_{\eta R_{\iota}}}^{loc}}{\overline{W_{pk}}} \tag{5}$$

Here $\overline{W_{pk}}$ is calculated using Eq. 6.

$$\overline{W_{pk}} = \sum_{i=XA}^{XP} \overline{A_{\eta R_{\iota}}}^{loc} \tag{6}$$

4. COMPARISON AND ASSESMENT OF OBJECTIVE AND SUBJECTIVE WORKLOAD

In this section, the subjective BWRS ratings assigned by all the TPs are compared with the objective metrics ($A_{\eta RC}$) outlined in Section 3 for each of the two phases of interest for the autorotation manoeuvre. Specifically, two objective metrics obtained from the $A_{\eta RC}$ are used for the comparison. First, the average value of the $A_{\eta RC}$ for each flight phase $A_{\eta RC}^{avg}$, and second the peak value of the $A_{\eta RC}$ for each flight phase, $A_{\eta RC}^{pk}$ is used.

4.1. Engine failure to stabilisation flight phase

Figure 5 and Figure 6 show the BWRS ratings awarded by each pilot. These are plotted against the respective metrics $A_{\eta RC}^{avg}$ and $A_{\eta RC}^{pk}$ defined in Section 3.

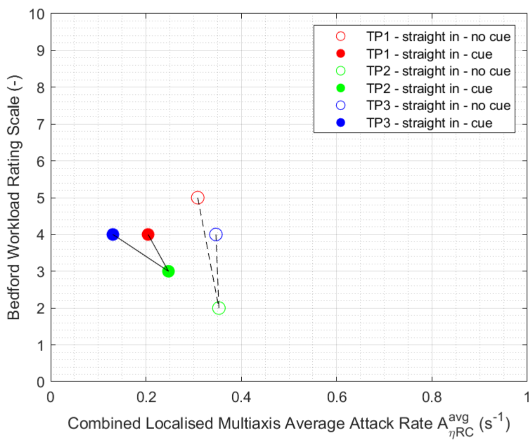

(a) Straight in.

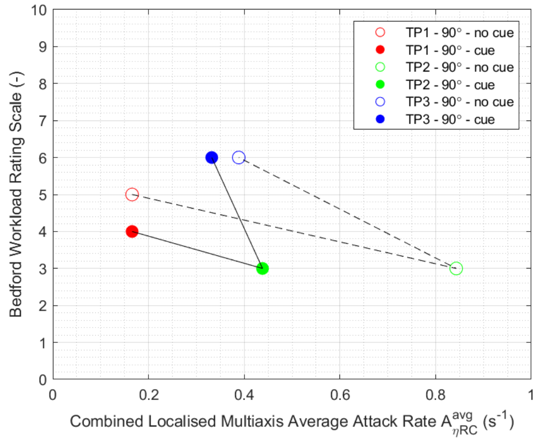

(b) 90^o turn to land.

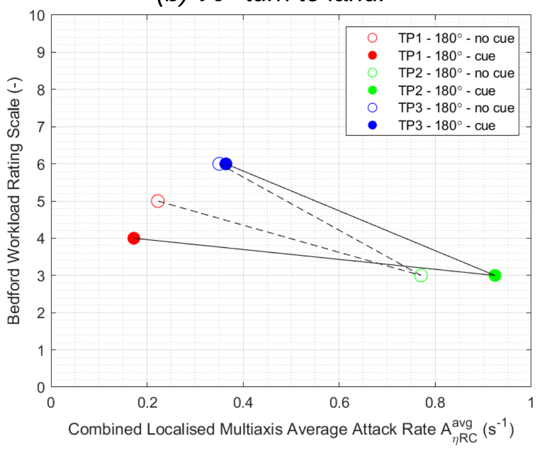

(c) 180^o turn to land.

Figure 5. Subject Bedford workload against average $A_{\eta RC}^{avg}$ combined localised multi-axis attack rate for engine fail to stabilise phase.

Reference [4] reported that, in general, when no cueing was provided to them, all of the TPs reported a higher subjective workload compared for the tasks with turns compared to the straight-in manoeuvre. This is to be expected and is reflected in the results of Figure 5. The subjective rating shows that the haptic cues only helped TP1 to reduce the reported workload. In fact, TP2 reported a higher workload for straight in when aided with cue. This reason can be related to the TP's comment that, "*It was annoying to have the XB stick shaker turned on as soon as the engine was failed*". A similar comment was provided by TP3 for the XB stick shaker coming-on as soon as the engine was failed.

The average $A_{\eta RC}^{avg}$, in most of the cases, shows that the average activity rate of the TPs is reduced with haptic cueing compared to the no cue case, except for the case of TP2 for 180^o turn to land. This may be explained further by TP2's comments, "*the roll angle pointer on the instrument panel was not very usable* *and I had to adjust the control stick position to learn how the roll angle pointer works, additionally I had to interact with the haptic cueing, so I had to make more control adjustments*". TP2 did not repeat the run before awarding the workload rating. This may have been the reason for $A^{avg}_{\eta RC}$ of TP2 with cue being larger than without the cue for the 180^o turn to land case.

It is interesting to note that the form of the 'curves' shown in the data is the same in each case in Figure 5, irrespective of the manoeuvre performed. That is to say that TP1 and TP3 tend to have higher workload and lower activity rates than TP2. If these TPs were taken in isolation on Figure 5(b) and (c), the (limited) data would start to support the hypothesis that subjective workload is positively correlated with the average attack rate for the pilot. However, Figure 5(a) and the addition of TP2 do not fit this hypothesis.

Figure 6 shows relationship between the subjective workload with respect to the peak attack rate, $A^{pk}_{\eta RC}$. It shows similar trends to Figure 5. In general, TP1 and TP3 report higher workloads for lower peak attack rates, $A^{pk}_{\eta RC}$ in comparison to TP2. This perhaps points to differing flying styles as well as different perceptions and/or interpretations of the terms in use in the BWRS. In addition to the objective measure, Figure 5 and Figure 6 gives an idea on each TP's flying style. For example, in Figure 6b and 5c, TP2 has a large peak value without any cue compared other TPs.

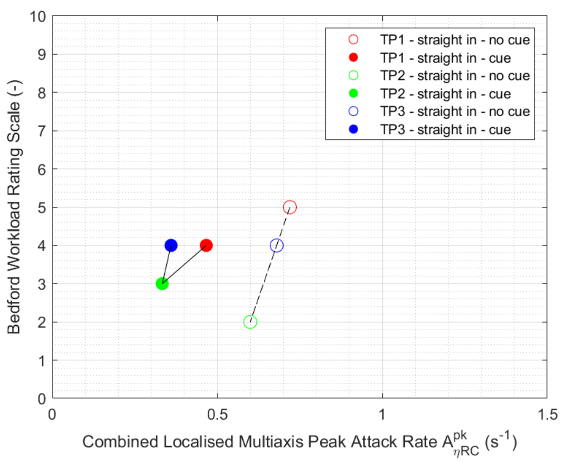

(a) Straight in.

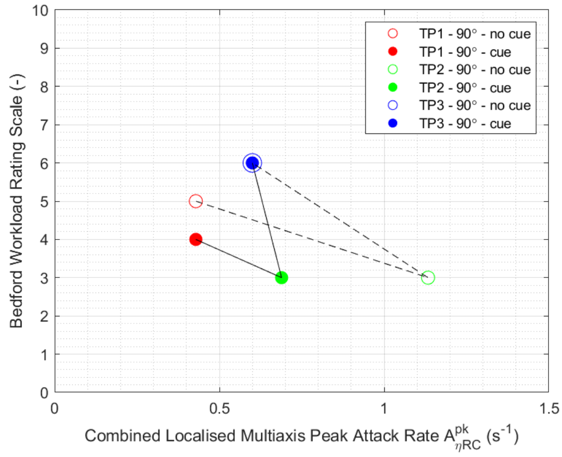

(b) 90^o turn to land.

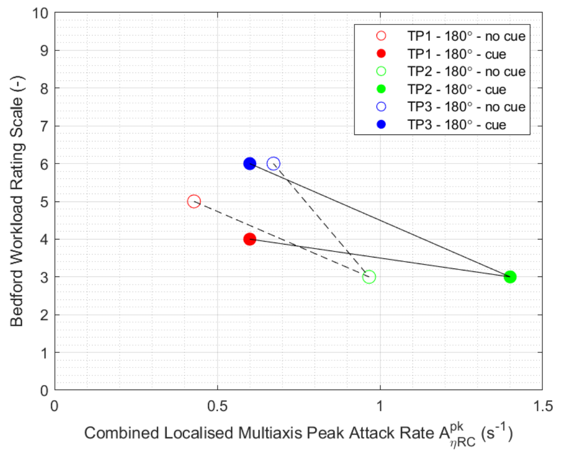

(c) 180^o turn to land.

Figure 6. Subject Bedford workload against peak $A^{pk}_{\eta RC}$ combined localised multi-axis attack rate for engine fail to stabilise phase.

This means TP2 provides a small and slow control input as soon as the engine failure is detected for the 90^o and 180^o turn to land cases. See Figure 7 for a comparison of the pilot's inputs for the 90^o turn without cue case. From Figure 7d, it can be seen that TP2 provided a more smooth and slower pedal (XP) input during the engine fail to stabilisation phase (red sections in the plot) compared to TP1 and TP3. However, from Figure 7b and Figure 7e (zoomed in plots, marked with circle), it can be seen that TP2 is providing constant low amplitude corrective inputs in the XB channel from around 7 to 15 seconds, causing the combined $A^{avg}_{\eta RC}$ to be large.

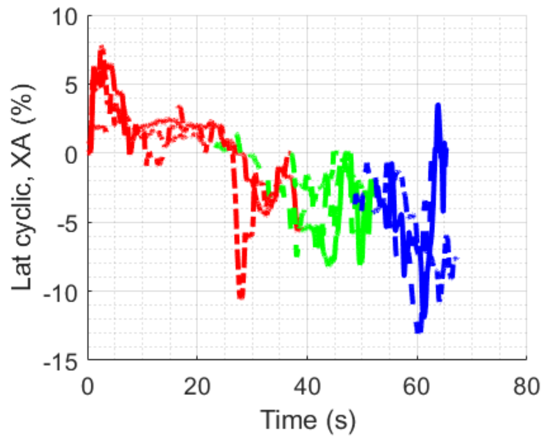

(a) Lateral cyclic input, XA.

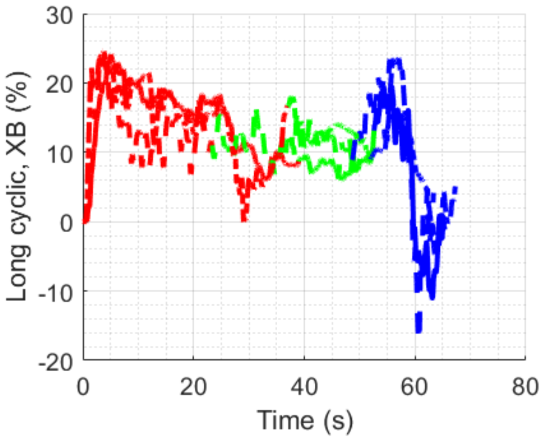

(b) Longitudinal cyclic input, XB.

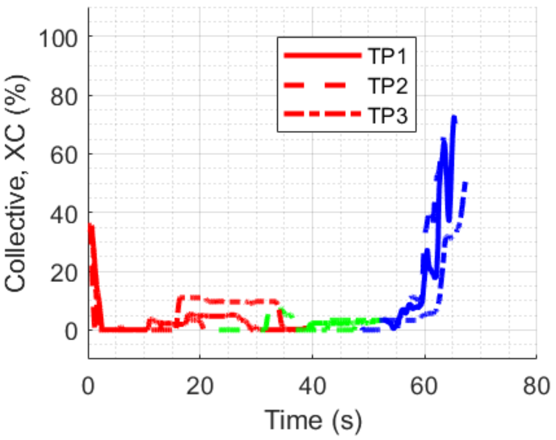

(c) Collective, XC.

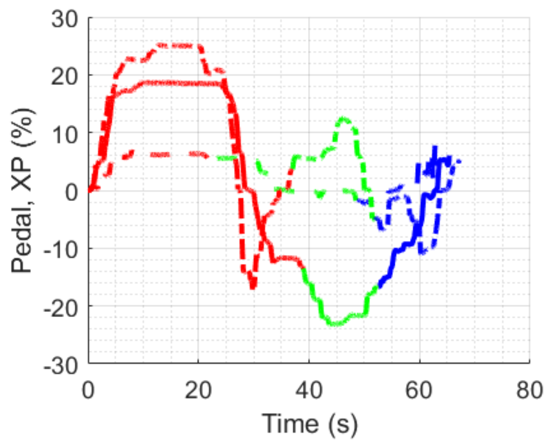

(d) Pedal, XP.

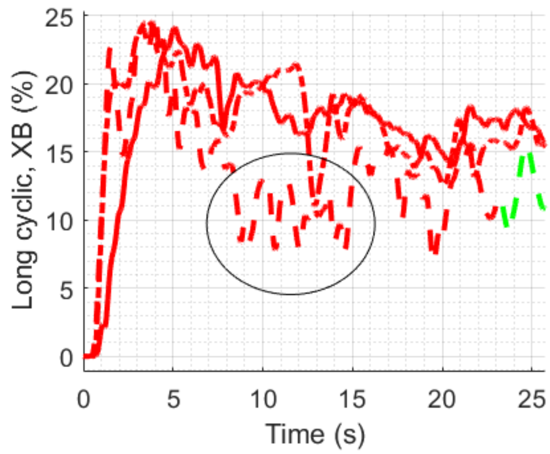

(e) Zoomed in XB plot.

Figure 7. Pilot's control inputs for 90^o turn without cue.

4.2. Steady state descent phase

Figure 8 and Figure 9 show the BWRS ratings awarded by the TPs in the steady state descent phase with respect to the objective metrics computed for the same task.

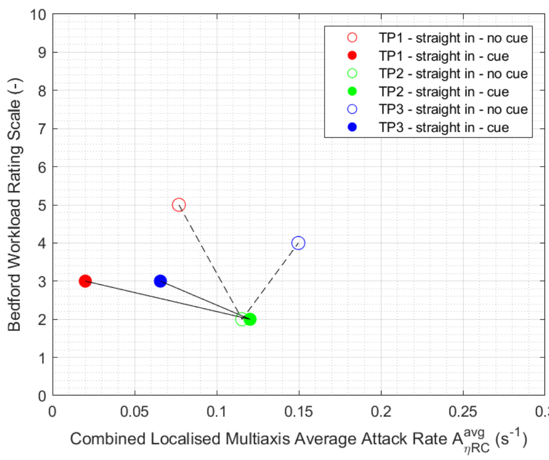

(a) Straight in.

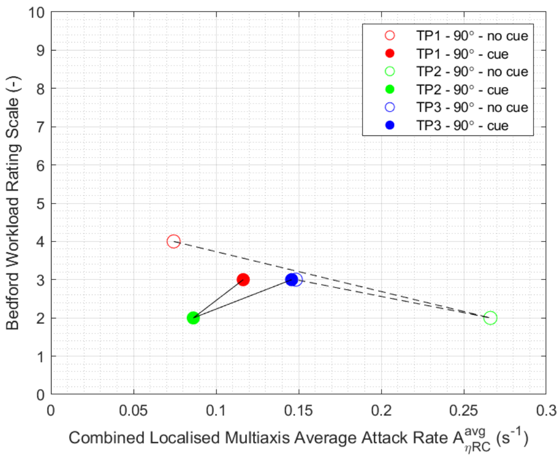

(b) 90^o turn to land.

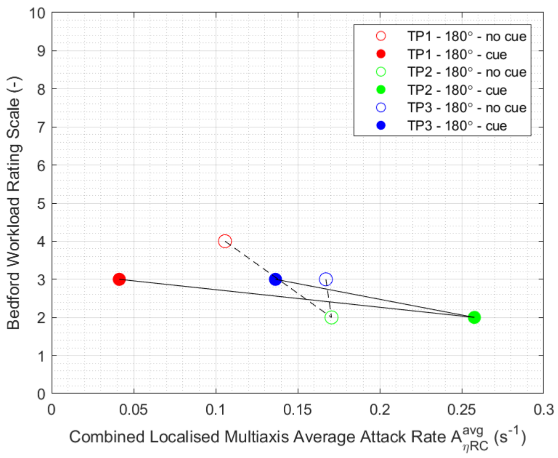

(c) 180^o turn to land.

Figure 8. Subject Bedford workload correlation with average $A^{avg}_{\eta RC}$ combined localised multi-axis attack rate for steady state descent phase.

Reference. [4] reported that, as might be expected, without cueing, all of the TPs reported lower subjective workload compared to engine failure to stabilisation phase. This is reflected in the result of Figure *8*. The subjective workload ratings show that the haptic cueing resulted in reduced reported workload from TP1 and TP3. However, the workload reported by TP2 remained unaffected by the cueing for the straight-in autorotation test case. It is posited that the workload for TP2 was not changed because TP2 was always within the bounds of the haptic cue shaker, meaning that the shaker was never activated. For the 90^o and 180^o turn to land cases, the haptic cueing also did not help TP2 and TP3 in reducing the reported workload. This can be explained by some exemplar TP comments: "*the 90^o turn was very tight, so the pilot had to work hard to line up with the runway and the manoeuvre became 'S-shaped'*". Also, the pilots reported that, "*very few sections of the flight in the steady state phase were available to fully exploit the haptic cue*".

It can be seen in Figure 8 that the average $A_{\eta RC}$ in the steady state descent phase is lower than the engine fail to stabilisation phase shown in Figure *5*. This is to be expected in the steady state phase assuming a well-trimmed descent where large control inputs are not constantly required to maintain the desired trajectory.

The form of the results is now somewhat different to those presented for the stabilisation phase of the manoeuvre. TP2 does not now always have the highest attack rate, for example. What is consistent is that the results do not appear to support the hypothesis that the attack rate parameter is well correlated with the subjectively reported BWRS workload rating.

Figure 9 shows relationship between the subjective Bedford workload ratings with respect to the peak $A_{\eta RC}$ for the steady state descent phase.

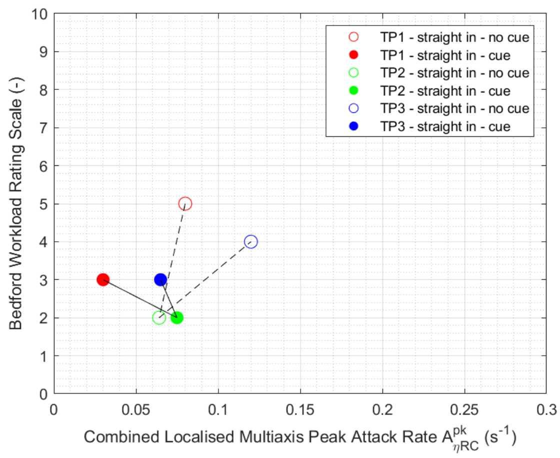

(a) Straight in.

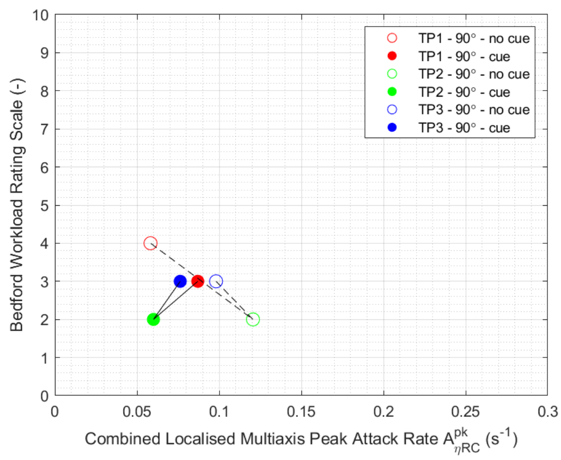

(b) 90^o turn to land.

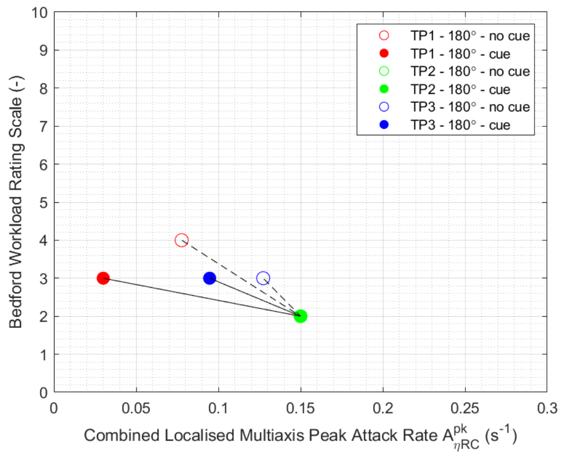

(c) 180^o turn to land.

Figure 9. Subject Bedford workload correlation with peak $A^{pk}_{\eta RC}$ combined localised multi-axis attack rate for steady state phase.

It can be seen from Figure 8 and Figure 9 that the average and peak values of $A_{\eta RC}$ are close to each other for all corresponding test case manoeuvres. This indicates that the pilots were making only minor adjustments in the control channels to maintain the steady state phase.

The combined multi-axis average attack rate matric $A_{\eta RC}$ provides a good indication of the pilot's control activity but it does not provide evidence for a direct correlation with Bedford workload scare rating. As with the previous results, there is no clear or obvious correlation between the subjective workload ratings awarded and the corresponding average or peak multi-axis attack activity rate.

5. CONCLUSIONS AND FUTURE WORK

This paper has reported the investigation into the correlation between subjective and objective workload metrics for piloted simulation flights used to assessment a novel autorotation haptic cueing method. The subjective workload was collected using the Bedford Workload Rating Scale. The objective assessment was carried out using the weighted combined multi-axis attack activity rate. Three different initial start conditions for the autorotation manoeuvre with and without haptic cueing in a good visual environment condition were tested. It was hypothesised that the subjective workload ratings would be well correlated with one or both average or peak multi-axis attack activity rates for the phase of the manoeuvre under consideration. However, no correlation was found between either the combined multi-axis localised average or peak attack activity and the subjective workload reported by the test pilots.

Since the correlation between the combined metric and overall BWRS rating awarded was found to be poor, the combined metric can be divided into Primary and Secondary controls based on the pilot control compensation as reported in Ref [7]. This may help in understanding if the pilot workload ratings represented specific or dominant controls rather than all controls combined. The primary and secondary control channels required for this method can be identified using the time frequency domain localised attack activity rate. This will be investigated in a follow up study to this one.

Author contact:
Mushfiqul Alam: mushfiqul.alam@cranfield.ac.uk
Michael Jump: mjump1@liverpool.ac.uk

ACKNOWLEDGMENTS

The piloted flight simulations used in this research was funded by the U.S. Government under Agreement No. W911NF-20-1-0323. The U.S. Government is authorized to reproduce and distribute reprints for Government purposes notwithstanding any copyright notation thereon. The U.S. Government technical monitor is Mahendra Bhagwat. The views and conclusions contained in this document are those of the authors and should not be interpreted as representing the official policies, either expressed or implied, of the Aviation Development Directorate or the U.S. Government.

REFERENCES

[1] ADS-33E-PRF, "Aeronautical Design Standard Performance Specification Handling Qualities Requirements For Military Rotorcraft," Redstone, Arsenal, Alabama, 2000.

[2] "DETERMINATION OF SHERIFF PRINCIPAL C D TURNBULL," Glasgow, 2019. https://doi.org/GLW-B1473-18

[3] Alam, M., Jump, M., and Rogers, J., "Simulated Flight Trial Assessment of Novel Autorotation Cueing Methods Using a Head Down Display," 2023. https://doi.org/10.4050/f-0079-2023-18027

[4] Alam, M., Jump, M., and Roger, J., "Further Simulated Flight Trial Assessment of Novel Autorotation Cueing Methods ," 2022.

[5] Alam, M., Jump, M., Eberle, B., and Rogers, J., "Flight Simulation Assessment of Autorotation Algorithms and Cues," 2020.

[6] Roscoe, A. H., and Ellis, G. A., "A Subjective Rating Scale for Assessing Pilot Workload in Flight: A Decade of Practical Use," *Royal Aerospace Establishment*, 1990, pp. 1–18. https://apps.dtic.mil/dtic/tr/fulltext/u2/a227864.pdf

[7] Memon, W. A., White, M. D., Padfield, G. D., Cameron, N., and Lu, L., "Helicopter Handling Qualities: A Study in Pilot Control Compensation," *Aeronautical Journal*, Vol. 126, No. 1295, 2022. https://doi.org/10.1017/aer.2021.87

[8] Blanken, C. L., Hoh, R. H., Mitchell, D. G., and Key, D. L., "Test Guide for ADS-33E-PRF," *HA1 Technical Report No. 1130-1*, 2008.

[9] Padfield, G. D., Charlton, M. T., Ehowell, S., and Rbradley++, J., "Paper Nr: 83 Where Does The Workload Go When Pilots Attack Manoeuvres? An Analysis Of Results From Flying Qualities Theory And Experiment." Retrieved 6 March 2024

[10] White, M. D., Perfect, P., Padfield, G. D., Gubbels, A. W., and Berryman, A. C., "Acceptance Testing and Commissioning of a Flight Simulator for Rotorcraft Simulation Fidelity Research," *Proceedings of the Institution of Mechanical Engineers, Part G: Journal of Aerospace Engineering*, 2013. https://doi.org/10.1177/0954410012439816

[11] Rogers, J., Strickland, L., Repola, C., Jump, M., Cameron, N., and Fell, T., "Handling Qualities Assessment of a Pilot Cueing System for Autorotation Maneuvers," 2017.

[12] Padfield, G. D., Clark, G., and Taghizad, A., "How Long Do Pilots Look Forward? Prospective Visual Guidance in Terrain-Hugging Flight," *Journal of the American Helicopter Society*, Vol. 52, No. 2, 2007, pp. 134–145. https://doi.org/10.4050/JAHS.52.134

[13] Tritschler, J. K., O'Connor, J. C., Holder, J. M., Klyde, D. H., and Lampton, A. K., "Interpreting Time-Frequency Analyses of Pilot Control Activity in ADS-33E Mission Task Elements," 2017.

APPENDICES

A. Bedford Workload Rating Scale

Figure A1 shows the Bedford Workload Rating Scale.

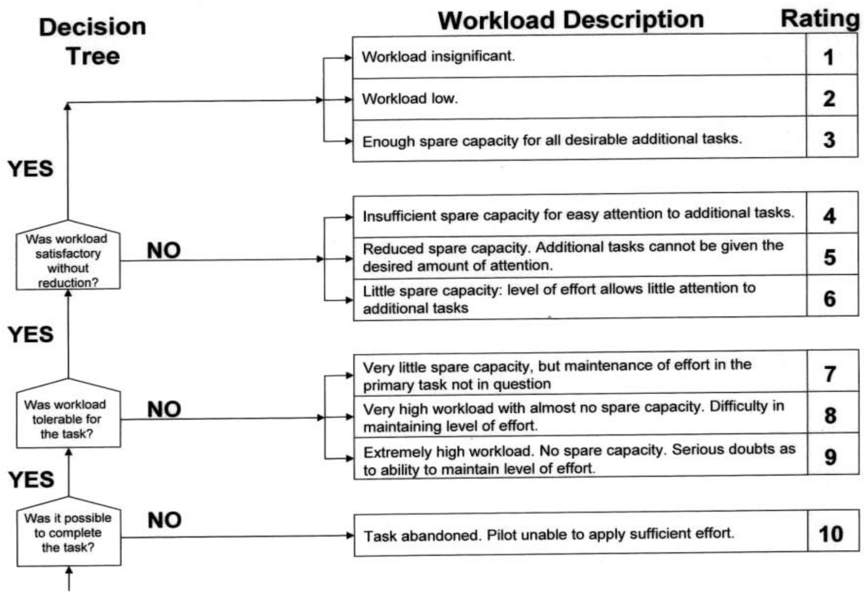

Figure A1. Bedford Workload Rating Scale.

B. Example Aircraft States

Figure B1 shows example aircraft state for TP1 during the autorotation manoeuvre while making a 90^o turn to land without any cues.

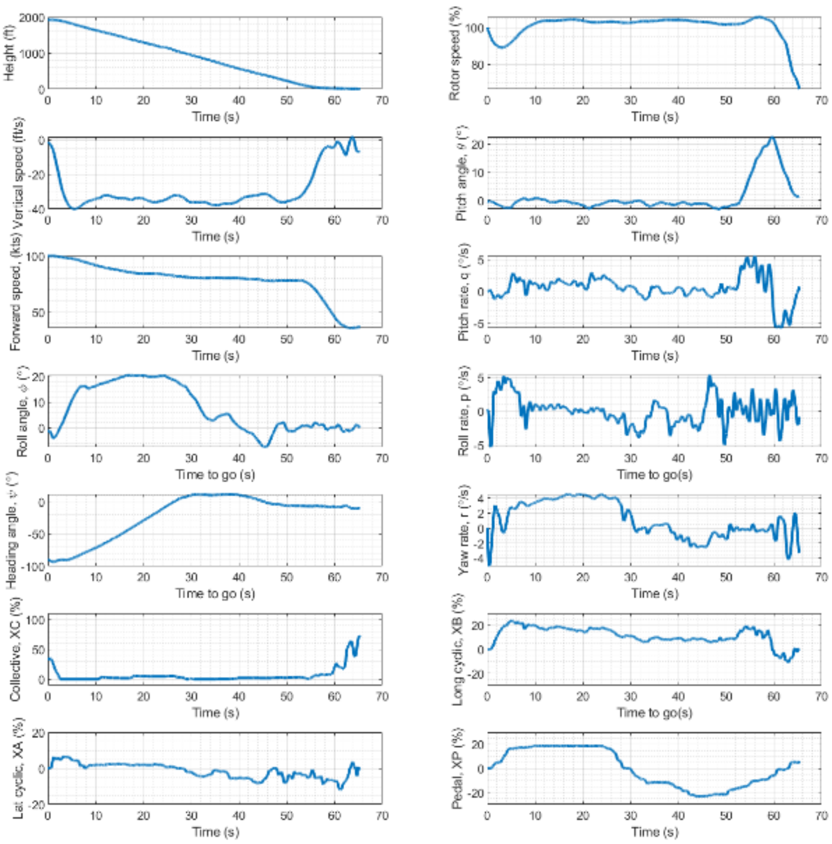

Figure B1. Aircraft states for the example autorotation manoeuvre to TP1.